INVESTIGATION LEADS TO IMPROVED UNDERSTANDING OF SPACE SHUTTLE RSRM INTERNAL INSULATION JOINTS

B. B. McWhorter, D. E. Bolton, S. V. Hicken, L. D. Allred, D. J. Cook
ATK Thiokol Propulsion Corp., Brigham City, UT

ABSTRACT

The Space Shuttle Reusable Solid Rocket Motor (RSRM) uses an internal insulation "J-joint" design for the mated insulation interface between two assembled RSRM segments. In this assembled (mated) segment configuration, this J-joint design serves as a thermal barrier to prevent hot gases from affecting the case field joint metal surfaces and O-rings. A pressure sensitive adhesive (PSA) provides some adhesion between the two mated insulation surfaces. In 1995, after extensive testing, a new ODC-free PSA (free of ozone depleting chemicals) was selected for flight on RSRM-55 (STS-78). Post-flight inspection revealed that the J-joint, equipped with the new ODC-free PSA, did not perform well. Hot gas seeped inside the J-joint interface. Although not a flight safety threat, the J-joint hot gas intrusion on RSRM-55 was a mystery to the investigators since the PSA had previously worked well on a full-scale static test. A team was assembled to study the J-joint and PSA further. All J-joint design parameters, measured data, and historical performance data were re-reviewed and evaluated by subscale testing and analysis. Although both the ODC-free and old PSA were weakened by humidity, the ODC-free PSA strength was lower to start with. Another RSRM full-scale static test was conducted in 1998 and intentionally duplicated the gas intrusion. This test, along with many concurring tests, showed that if a J-joint was 1) mated with the new ODC-free PSA, 2) exposed to a history of high humidity (Kennedy Space Center levels), and 3) also a joint which experienced significant but normal joint motion (J-joint deformation resulting from motor pressurization dynamics) then that J-joint would open (allow gas intrusion) during motor operation. When all of the data from the analyses, subscale tests, and full-scale tests were considered together, a theory emerged. Most of the joint motion on the RSRM occurs early in motor operation at which point the J-joints are pulled into tension. If the new PSA has been weakened due to humidity, then the J-joint will partially pull apart (inboard side), and the J-joint surfaces will be charred by exposure to hot gases. After early operation, a J-joint that has been pulled apart will come back together as the J-joint deformation decreases. This J-joint heating event is relatively short and occurs only during the first part of motor operation. Internal instrumentation was developed for another full-scale static test in February 2000. The static test instrumentation did indeed prove this theory to be correct. Post-test inspection revealed very similar charring characteristics as observed on RSRM-55. This experience of the development of a new PSA, its testing, the RSRM-55 flight, followed by the J-joint investigation led to good "lessons learned" and to an additional fundamental understanding of the RSRM J-joint function.

INTRODUCTION AND BACKGROUND

This paper presents an investigation into an internal rubber joint of the Space Shuttle Reusable Solid Rocket Motor (RSRM). Before the explanation of this rubber joint is given, some basic background information regarding the RSRM assembly will be given here. The RSRM is composed of four segments. These four segments are assembled, or mated, to form a full length RSRM. The assembly of the four segments makes three "field joints" between the segments. Each field joint is composed of a "tang" and "clevis", which are the mated parts of steel case ends. Each case field joint is sealed by two O-rings. This design is a redundant sealing system.

There are two other features in the joint design that serve as thermal barriers to this redundant sealing system. These features are a "capture feature" O-ring and an internal insulation "J-joint" configuration. This internal insulation J-joint design is the configuration for the mated rubber insulation interface between two assembled RSRM segments (see Figure 1). Since there are three field joints, there are also three J-joints - forward, center, and aft.

This J-joint design is the first thermal barrier that prevents hot gases from affecting the case field joint metal surfaces and O-rings.

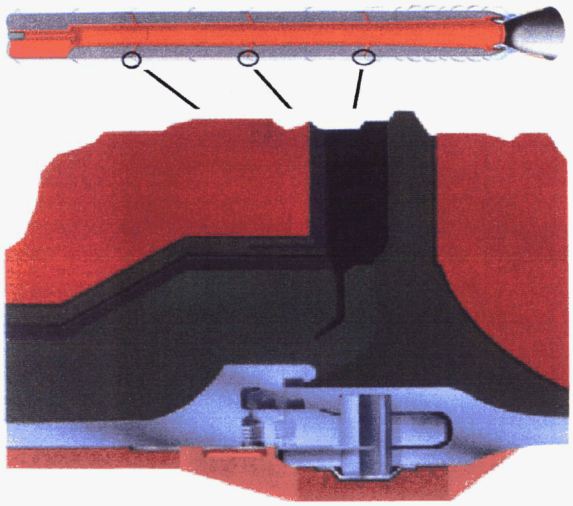

Figure 1. Assembled RSRM Showing Internal Insulation J-joint Configuration for the Three Field Joints

In this assembled (mated) segment configuration, this rubber J-joint design serves well as a barrier to hot gases. It works so well, in fact, that the J-joint almost acts as a seal, but it is not officially considered a seal. Since the J-joint is composed of internal rubber insulation, this component can be visualized as two rubber parts joined together, or pressed against each other, in the assembled RSRM configuration. On one side of the interface is the rubber insulation part referred to as the "J-leg" (see Figure 1). On the other side is the rubber insulation part referred to as the "clevis". (Hereafter in this paper, the term "J-joint" applies to the mated configuration of these rubber components.)

Three aspects of the J-joint design enable it to be an effective gas barrier: 1) the mated joint makes an interference fit, 2) the configuration of the J-joint enables the internal motor gas pressure, at least partially, to produce a pressure actuated seal between the two mated insulation surfaces, and 3) a pressure sensitive adhesive (PSA) provides some structural adhesion between the two mated insulation surfaces.

SELECTION OF A NEW PSA

In 1995, selection of a new environmentally friendly PSA was initiated. The desired new PSA was to be free of ozone depleting chemicals (ODC-free). After subscale testing of several PSA types, a new ODC-free PSA was selected. Its strength was less than the old PSA. However, it was thought that the interference fit and pressure actuation of the J-joint design were the controlling parameters that made the J-joint an effective hot gas barrier. The ODC-free PSA was successfully tested on an RSRM full-scale static test (referred to as FSM-5). Armed with this success, the new ODC-free PSA was selected for flight on STS-78. The flight set of solid rocket motors for STS-78 was "RSRM-55". (The remainder of this report will refer to this solid rocket motor flight set as "RSRM-55". The new ODC-free PSA will be referred to as the "new PSA" hereafter in this report.)

THE PROBLEM

The flight occurred as planned. Post-flight inspection revealed that the J-joints, assembled with the new PSA, did not perform well. Hot gas had seeped into the J-joint interfaces. The inboard portions of the J-joint interface surfaces were heavily heat affected and charred on four of the six joints (there are two motors for each flight set - hence six total field joints). The four severely affected J-joints were the aft and center J-joints for each motor. The forward J-joints were only slightly heat affected or sooted in four small areas. Figure 2 illustrates with a cross-section schematic where the severe charring was located. Figures 3 and 4 show example photos of the heat affected J-joint mating surfaces. As shown in Figure 2, the heat effect and charring of the rubber interface surfaces were limited to only the J-joint surfaces inboard of the radius start. Although the J-joints did not perform as intended, their outboard (outer diameter) interfaces appeared to have remained closed and did work as a thermal barrier (this region is also identified in Figure 2). No joint metal or O-rings were affected by hot gas. Some soot did penetrate past the radius start on at least one of the joints, but this joint still served well as a thermal barrier.

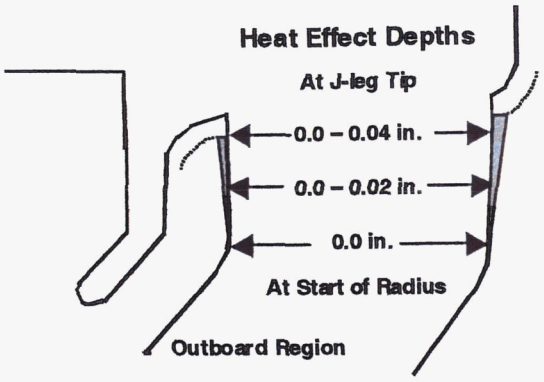

Figure 2. Heat Effect and Char on the J-joint Interface Surfaces of RSRM-55

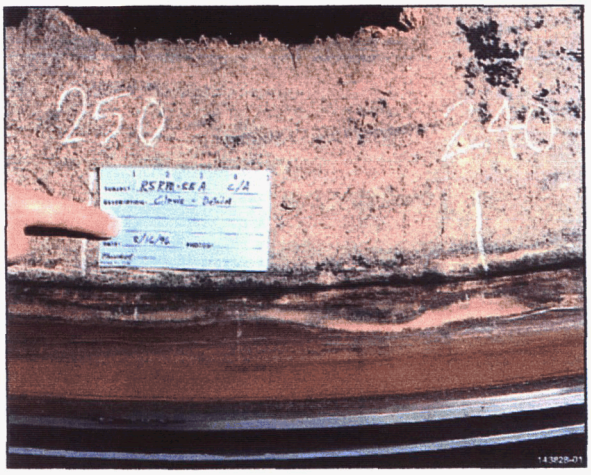

Figure 3. Photograph of Heat-Affected and Charred J-joint Surface From RSRM-55

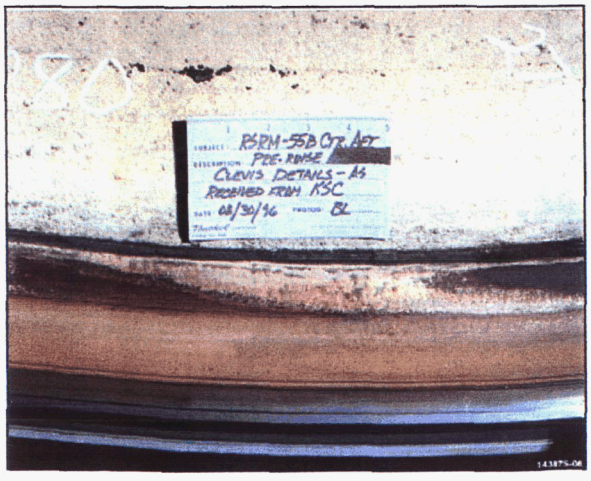

Figure 4. Photograph of Heat-Affected and Charred J-joint Surface from RSRM-55

Although no heat reached the O-rings or metal surfaces, this J-joint gas intrusion was a first time ever occurrence in the RSRM program. RSRM motors had been flown over 100 times before with no PSA failure. The J-joint gas intrusion on RSRM-55 was a mystery to the investigators since the new PSA had previously worked well on the FSM-5 full-scale static test. Compounding the problem further, the forward J-joints of RSRM-55 experienced only minor heating in a few small areas, whereas the center and aft J-joints were heat affected extensively.

INITIAL INVESTIGATION

A team was quickly assembled to study the J-joint, PSA, and all other materials and processes. The evidence confronting the team was perplexing. A first impression was that the new PSA somehow caused the J-joint to have gas intrusions. However, the testing that was done for the new PSA would suggest that the new PSA could not be the cause for gas intrusion. It was true that the only obvious change to the J-joint mating process was the adoption of the new PSA and ODC-free cleaning process. But, the following were also true:

1) The "new" PSA had been tested on the aft J-joint of the FSM-5 motor successfully. During normal operation, this aft joint insulation experiences the most severe heating effects and thermal ablation compared to the other joints. So logically, it was thought that this joint would provide the most conservative test bed for the J-joint and PSA system.

2) Lab tests had shown that the strength of the new PSA was lower than the old PSA. However, the design of the J-joint was such that it was thought to be pressure actuated. In other words, the J-leg should remain seated to the opposite clevis side of the joint by motor chamber gas pressure. Under this assumption, the J-leg should remain seated to the clevis even while the clevis is experiencing deformation due to the chamber pressure. Figure 5 illustrates this deformation under motor chamber pressure and how the J-leg will move with the clevis and thereby remain seated to the clevis in this condition. Therefore, the reduction in PSA strength was not considered an important factor.

3) When the segments are mated, an interference fit is produced between the J-leg and clevis. This interference fit should allow the J-leg to remain in contact with the clevis during the prelaunch time frame. The J-leg-to-clevis interface should never go into tension during prelaunch.

4) Over 100 RSRM motors had either flown or had been static tested with the "old" PSA, and no heat effects were ever observed in a normal rubber interface of the J-joint (this statement does not include static tests in which intentional flaws were created in the J-joint to study the various aspects of joint performance)

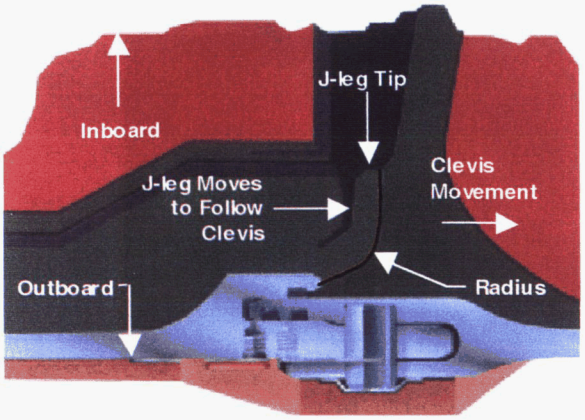

Figure 5. J-joint Configuration During Motor Operation

Since the initial investigation revealed contradictory evidence that the new PSA caused the gas intrusion, nothing was assumed. Broader questions were addressed. Was there another material, joint dynamic, assembly process, or motor performance parameter that caused the J-joint gas intrusion? Was an undetected bad lot of a material used in manufacturing? Did the motor internal operational heating environment change? Did something in processing change - such as transportation in an unusually rough or cold environment? When did the J-joints opening and the heating occur? Were the J-joints opened at ignition or prior to ignition? Or, could an unusual post-operation event during re-entry have caused the J-joints to open and then become heat affected?

An extensive fault tree was developed. The fault tree did not assume that the J-joint gas intrusion was due to the application of the new PSA. Instead, all possible root causes for the event were considered. The fault tree branched into four major categories of causes, and each of those causes were subdivided further and those cause were divided until a possible root cause could be postulated. The four major areas for defining causes were 1) a motor performance parameter caused these J-joints to open; 2) some different joint dynamics were encountered which caused the J-joints to open; 3) inadequate materials (other than the PSA) were installed prior to the joint assembly; and 4) the J-joint assembly process, including use of the new PSA and ODC-free process, was inadequate.

Material and fabrication records were reviewed to determine if any manufacturing material or process changes could have triggered the J-joint problem. Processes at Kennedy Space Center (KSC) were reviewed. All procedures were in agreement with Thiokol and KSC requirements. No changes were found that could have affected the J-joint – except for, the incorporation of the new PSA.

The RSRM-55 J-joints were studied to insure that their configuration was within family. Preflight inspection data was studied. There was normal axial engagement during assembly to produce the desired interference fit between each J-leg and corresponding clevis. Photos and samples of the post-flight J-joints were studied. The condition of the mated surfaces were observed and measured. The heat affected regions of the J-joints were mapped and recorded. Other than the anomalous heat affected rubber, the J-joints were normal.

Lab analysis of the samples revealed that the heat effect was severe and resulted from material temperatures exceeding 1800°F. The char (complete material thermal decomposition) depth on the J-leg and clevis surfaces varied from 0 to 40 mils (Figures 3 and 4). J-joint insulation char was only observed along the J-joint surfaces inboard of the J-joint radius (Figure 2).

In conjunction with the hardware study, the environments to which RSRM-55 hardware was exposed were studied. No data was found that indicated that the RSRM experienced anything other than a normal flight environment. Vibration and temperature records during transportation were normal. Processing environments were within family.

An ODC-free cleaning process for the J-joint had also been added to the assembly. However, lab tests showed that the ODC cleaning process had no adverse effects on the J-joint or PSA.

A re-examination of post-flight history data was made so that the condition of RSRM-55 could be compared and contrasted to earlier post-flight data. Much of this data are thickness measurements of the

remaining insulation components. Internal insulation is ablated and eroded during flight. Thickness measurements of the remaining insulation components are made for every flight. The remaining inboard thickness of the J-joint rubber components, including the J-leg and clevis, were within family. The thickness measurements of all other internal insulation components, such as propellant grain inhibitors and stress relief flaps, were within family. The case insulation thermal decomposition depths were within family. This review of post-flight data concluded that all of the measurements and observations of RSRM-55 were within family, except for the anomalous J-joint heat effects already under investigation. No other similar heat effects had been observed prior to RSRM-55.

Reviews were conducted of earlier certification static tests in which the J-joints were flawed to demonstrate the robust RSRM field joint design. One full-scale test, QM-6, incorporated a "wave defect" which did result in heat effect and sooting patterns similar to those measured on RSRM-55. In QM-6, the wave defect was made so that the J-leg and clevis did not contact for a circumference of several inches. The remainder of the joint was normal. Post-test inspection revealed heat affected rubber in the wave defect region. In this region, soot patterns were very similar to those patterns on RSRM-55. Obviously, this early certification test, performed with a flawed J-joint and with the older and stronger PSA, produced heating characteristics that were similar to RSRM-55. However, RSRM-55 had no wave defect flaws, and all data indicated that the shape of the J-joints were normal.

The design background of the J-joint was reviewed. A structural analysis done earlier showed that the high pressure gas during motor operation would force the J-leg against the clevis - the J-joint was pressure actuated. Under this loading, the strength reduction of the PSA should not be a cause for J-joint opening. It was concluded that the prelaunch and flight environment must have introduced another, and as of yet, unknown variable into the physics of the J-joint and PSA operation.

Detailed Investigation - Root Cause and Timing

Obviously, there were some other combinations of physics at work that prevented the new PSA from functioning properly in the J-joint. Testing of the new PSA, prior to its incorporation into the RSRM-55, had been thought to be conservative and thorough. Since the root causes for J-joint gas intrusion were not understood, the team concluded that the prior PSA testing had been missing something. As RSRM production resumed using the old, proven PSA, the investigation team now concentrated on a longer and more in-depth study of the J-joint and PSA physics. The other variables causing the gas intrusion needed to be understood before another new ODC-free PSA or modified PSA could be considered for the RSRM program.

In addition to the fault tree, an event tree was developed. The event tree laid out all RSRM events, non-operational and operational, from pre-ignition through splashdown. The purpose of this event tree was to define the timing for the opening and subsequent heating of the J-joint. As studies of all possible root causes of failures were conducted, the scenarios that could provide the thermal and structural boundary conditions to create the J-joint heating effects were also studied. All events were investigated – including motor bending due to ignition of the shuttle main engines, RSRM ignition, and all other operating phases of the RSRM. Events prior to motor operation as well as post-motor operation, such as re-entry events, were considered. As the investigation proceeded into the many possible root causes defined by the fault tree, evidence that either supported or refuted an event time for the gas intrusion was formed. With this information, the event tree table was filled, and likely scenarios that would create a J-joint gas intrusion emerged.

This continued in-depth study reviewed many hypotheses. With each new hypothesis, other possible variables of the physics were considered. Subscale testing, lab testing, and analysis were conducted to determine the merit of these hypotheses. In the end, two other variables, one for a storage condition and the other for an operation condition, were determined to be important. As with most unexpected events, a combination of root causes would explain this PSA failure and J-joint gas intrusion.

Humidity

PSA strength tests had already been completed prior to RSRM-55. The new PSA strength had already been determined to be less than the old PSA strength.

But, the old assumptions of the operating physics allowed, in theory, a weak PSA to be acceptable. For the reasons stated above (interference fit and pressure actuation) it was thought that this strength parameter was not important.

In early tests, humidity had been included. Unfortunately, the exposures were for a short period of time and were only for the PSA application process. These tests showed no significant effect of humidity. Extended humidity exposure was not done for the J-joint rubber prior to the PSA application.

During the investigation, the strength tests were performed again, but this time, these tests were performed under different conditions. Samples were exposed to periods of humidity that would simulate the KSC conditions prior to joint assembly. PSA strength tests were conducted for a matrix of aged and humidified samples. The results showed that humidity exposure time was an important governing variable that adversely affected PSA strength.

Both old and new PSAs were adversely affected by aging in high humidity environments. However, since the strength of the old PSA started out higher, its strength remained higher in humid environments compared to the new PSA.

Extended humidity exposure effects were considered important since the new PSA had been certified and tested in Utah where the climate is dry. For flight motors, the J-joint rubber is exposed to long periods of high humidity prior to joint assembly as the segments are stored at KSC. After assembly, the PSA is weakened by this moisture. Although, believing the J-joint was pressure actuated during operation, the investigation team was confident that the weakening effects of humidity was an important variable in determining the root cause for the PSA failure.

JOINT MOTION

Another operating condition of the joint that had been studied during the design of the RSRM had to do with joint motion that occurs during motor operation. Joint motion had been studied thoroughly for case joint structural integrity and for proper O-ring operation. Exactly how joint motion might fit into to the physics of the J-joint and PSA failure, however, had not been as thoroughly studied.

Due to loads, dynamics, and the structure of the assembled motor, each field joint experiences somewhat different motion. Post-flight inspection of RSRM-55 revealed that the amount of heat effect in each J-joint strongly correlated to joint position – forward, center, or aft. There was little to insignificant heating in the forward J-joints on both motors. The center J-joints, however, were heavily heat affected and had the most char and sooting. The aft J-joints did experience severe heating and charring, but not as bad as the center J-joints.

During the investigation, conclusions of old structural analyses were revisited, and new analyses were conducted. The case joint motion was examined closely. During motor operation, the internal propellant grain deforms due to the gas pressure distribution across the surface of the grain. Also, the case membrane strains more than the case joint regions since there is extra thickness in the case joint. This elastic straining causes the case joints to rotate – that is, as the membrane on either side of the joint expands, the internal joint surface becomes slightly convex. This joint rotation, combined with the motion of the internal propellant grain deformation, results in a relative displacement between the two sides of the J-joint. The J-joint deforms and tends to go into tension as illustrated in Figure 5.

The amount of resulting axial displacement at the J-leg-to-clevis interface could not be precisely calculated. The combination of the visco-elastic properties of the propellant grain and rubber insulation components in response to the case deformation and internal pressurization is an extremely complicated problem. However, the available results showed that the forward field joint should experience the least amount of J-joint motion during operation. The center field joint experiences the most J-joint motion. The aft field joint experiences more motion than the forward, but not as much as the center J-joint. This variation in J-joint motion corresponded exactly with the varying amounts of heat effect observed in the J-joints of RSRM-55.

This correlation was too much of a coincidence not to have something to do with the physics that resulted in hot gas intrusion into the J-joints of RSRM-55. But again, the J-joint was thought to be completely pressure actuated during operation. In other words, internal gas pressure would force the J-leg against the moving clevis insulation. With

pressure actuation, the PSA did not have to be a strong adhesive. It was apparent that this joint physics needed to be reexamined.

INCOMPLETE PRESSURE ACTUATION

The re-analysis of this theory proved that the J-leg is not fully pressure actuated. Along the inboard portion of the J-leg, from the J-leg radius inboard to the J-leg tip (Figure 6), there is little to no pressure actuation. The reasons can be explained as follows:

Consider a J-joint assembled with an ineffective PSA. Upon J-joint assembly, there exists contact between the insulation clevis and J-leg (see Figure 6). Between the J-leg tip and radius, there exists a certain amount of free volume created by the shapes of the mating surfaces. This geometry was created intentionally to assure J-leg tip contact with the clevis and to assure an interference fit at assembly. When the J-leg is pressed into the clevis by motor gas pressure, the free volume is allowed to compress, as illustrated in Figure 7. The pressure of the free volume increases with this compression until static equilibrium is achieved at or near the pressure of the motor chamber. This situation now results in a J-leg with essentially the same pressure inside the joint as there is in the motor chamber. This is essentially equivalent to the condition just after assembly, before motor operation, when there is atmospheric pressure (14.7 psi) on both sides of the J-leg. Only now, during motor operation, there is roughly motor pressure on both sides of the J-leg. So contact pressure at the tip is approximately the same as it is just after assembly – hence no pressure actuation. In fact, due to clevis deformation during motor operation, as shown in Figure 7, the J-leg must be pulled away from its assembled position, and so there may be even less pressure where the J-leg tip contacts the clevis.

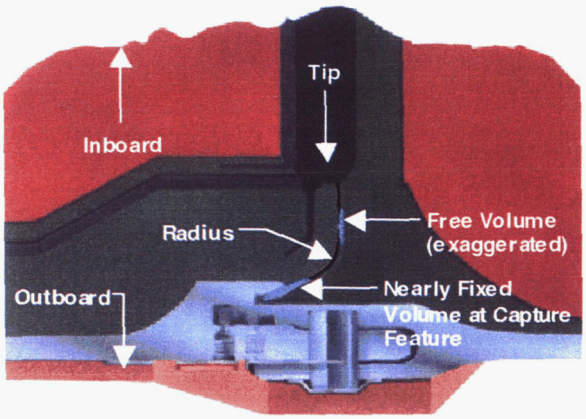

Figure 6. J-joint Assembled Configuration Prior to Motor Operation Showing Uncompressed Free Volume

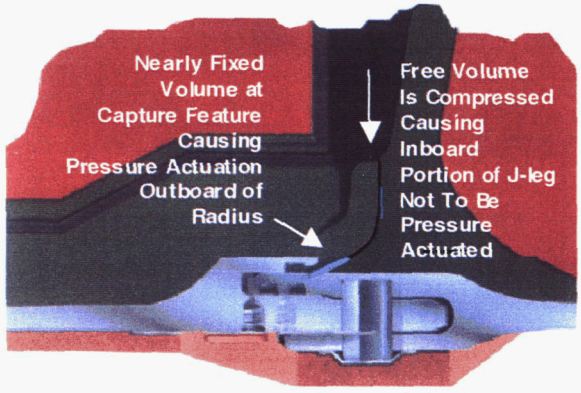

Figure 7. J-joint Deformation Configuration During Motor Operation Showing Compressed Free Volume

A key point here is the observation that the free volume geometry is such that it can be compressed as the J-leg rubber presses it. If the volume was fixed so that it would not be compressed, then the pressure in the free volume would remain at 1 atmosphere during motor operation. In that case pressure actuation may work.

For the region outboard of the radius, the condition of having a fixed volume is almost that situation. In Figure 6, the volume adjacent to the capture feature O-ring is surrounded by rigid case metal hardware. During motor pressurization, the J-leg rubber presses into this outboard volume somewhat. But mostly, the volume is controlled by the rigid surfaces of the case. Therefore, this region outboard of the J-leg radius is pressure actuated as illustrated in Figure 7. It remains pressure actuated whether the J-leg

inboard region remains in contact with the clevis side or not (Figures 8a and b).

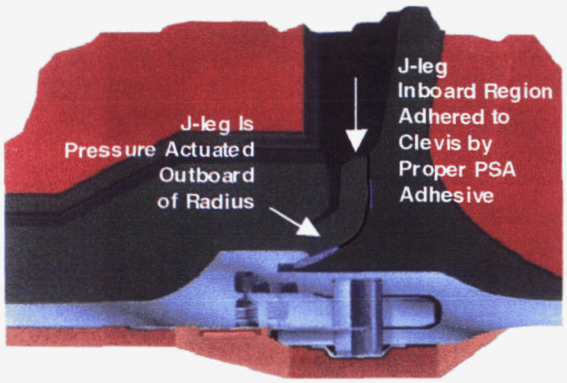

(a) Proper PSA Operation

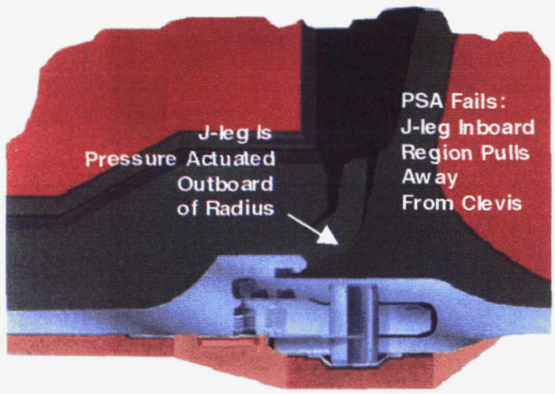

(b) Failed PSA

Figure 8. J-joint Deformation During Operation With Proper PSA Operation and With Failed PSA

A second advance in the understanding of the pressure actuation effects on the PSA was made in the laboratory. These tests involved tensile and peel testing rubber/PSA/rubber samples under high gas pressure and under only one atmosphere of pressure. It was noted that tensile buttons tended to have higher strengths under high gas pressure environments than under ambient pressure. This indicates that the rubber-to-rubber interface, with PSA but no volume, does tend to have some pressure actuation effect in tensile mode. This difference in strength was not observed for peel tests – there was no pressure actuation effect for peel modes. The important point to recognize is that if the failure mode is from the inside out (like a suction cup), then the pressure actuation effect of a rubber-to-rubber interface, with PSA, can be important. If, however, the failure mode peels from the edge to the inside (like peeling the edge of a suction cup away), then the pressure actuation of a rubber-to-rubber interface, with PSA, will not be effective.

In summary, the length of the J-leg from its radius inboard to its tip is not pressure actuated (refer back to Figure 7). The length of the J-leg outboard its radius, and including its radius region, is pressure actuated. During motor pressurization, the insulation clevis deforms due to joint rotation and propellant grain deformation. This motion tends to pull the J-leg towards the clevis. If the PSA is strong enough to hold it (Figure 8a), then the J-leg will maintain contact following pressure equilibrium. If, however, this clevis movement is significant and if the PSA has weak adhesive strength, the J-leg tip will peel away from the clevis (Figure 8b). The J-leg length outboard of the radius region, however, will be sucked into the clevis since motor chamber pressure will exceed the pressure in the volume in the capture feature region.

THE RSRM-55 PSA FAILURE THEORY

When all of the data from the analyses, sub-scale tests, FSM-5, and RSRM-55 were considered together, a theory emerged that combined the effects of 1) long term humidity exposure weakened PSA and 2) J-joint motion during operation with the correct physics of pressure actuation. It was postulated that pressure actuation by itself will not hold the J-joint together. The adhesive strength of the PSA is at least needed during a part of motor operation. It was postulated that the new PSA would be strong enough to work if the J-joint and PSA was affected by one of the two variables – humidity or significant joint motion – but not both.

PROOF FOR THE PSA FAILURE THEORY

Because of the complicated nature of the J-joint physics, the theory stated above could only be proven by use of a full-scale RSRM static test. The investigation team understood that one data point had already been gathered – the effects of joint motion alone. FSM-5 had demonstrated that the new PSA will work on an aft J-joint, which has significant motion. In that test, however, the J-joint/PSA system had not been exposed to higher humidity for extended times. This was the main data point that indicated that both humidity and joint motion were needed to fail the new PSA.

The investigation team decided that the next full-scale test (FSM-7) needed to demonstrate what would happen with both variables affecting the aft J-joint. So, the FSM-7 aft J-joint, using the new PSA and the ODC-free cleaning process, was also processed with a simulated KSC humidity (a process that targeted a simulated exposure of 60% to 80% relative humidity). This would make the aft J-joint experience the combined effects of humidity and joint motion. The investigation team felt that this would simulate as close as possible the aft J-joint on RSRM-55.

To further test that joint motion alone would not cause the PSA to fail, the center J-joint on FSM-7 was processed with the same variables but without humidity.

The forward J-joint, which experiences little J-joint motion, was assembled with long exposure to humidity. The new PSA was applied to one half of the J-joint surface, and the old PSA was applied to the other half. Both halves had partial flaws designed to allow hot gas to penetrate the J-joint well after motor ignition. The gas pressure would reach to the start of the radius region - but not beyond that point.

The FSM-7 results were conclusive. The post-test observations of the aft J-joint revealed strong heat effects, including charring, on the J-joint interface surfaces. The charring did not extend pass the radius, which tended to prove that the outboard portion of the J-joint was pressure actuated (similar to RSRM-55 aft J-joints). But the inboard portions of the aft J-joint were definitely exposed to heat during motor operation.

The center J-joint, meanwhile, was not heat affected at all. The new PSA held this joint together – in the joint that experiences the most J-joint motion.

The forward J-joints did not open or experience any heat effect – even with the partial intentional flaws.

The conclusions from this test were significant. The new PSA was failing during motor operation. This indicated that this heating event did not occur during re-entry, which of course, a static test motor does not experience. The new PSA would fail if the J-joint experienced both extended humidity exposure and significant joint motion.

Timing and Duration of the Heating Event

Now, the variables that caused new PSA to fail in the J-joint were understood. However, the exact timing for the failure was not known. The duration for which the J-joint was exposed to hot gas was not known. Thermal and structural analyses were used to approximate the answers to those questions.

Thermal Modeling Results

Thermal models were needed to reproduce the char configurations measured on RSRM-55. These models, if they accurately reproduced the char configurations, could then possibly address the timing and the duration of the J-joint hot gas intrusion.

Charred J-leg specimens were taken from RSRM-55. Cross-sections of the J-leg were made, and the char configurations were studied. Figure 9 shows a typical cross-section of an RSRM-55 J-leg. The J-leg mating surface is identified on the figure. In normal operation, this mating surface stays in contact with the clevis, so this surface would not be charred. In RSRM-55, the PSA failure allowed the J-joint to open thereby exposing this mating surface to heat. The char depth on this mating surface varied from 30 to 0 mils.

Under a charred surface is the pyrolysis zone. This is the material that has undergone heat decomposition but has not been fully converted to char (Char is material that is fully thermally decomposed and carbonized). In Figure 9, the depth of the pyrolysis zone at the mating surface is thin relative to the charred material indicating that the heating event was intense but short in duration.

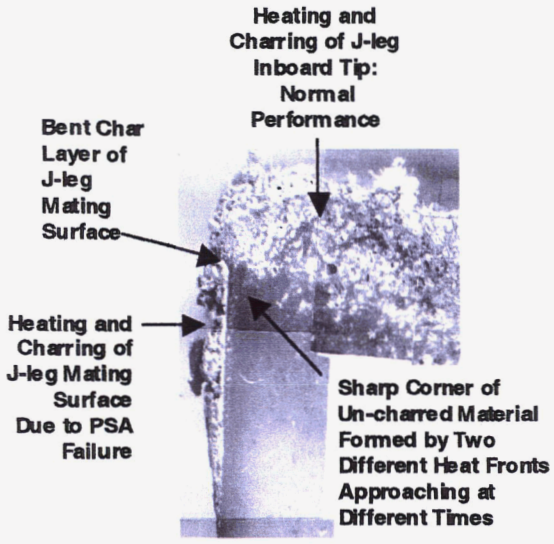

Figure 9. RSRM-55 J-leg Cross Section Showing Char Thickness

Also noted on this figure, is the typical J-leg tip char. This char results from normal motor operation heating of the J-leg inboard diameter surface. This char and heat affected depth varies from 0.2 inches to 0.4 inches from the original pre-fired inboard surface depending on J-joint location. When this J-leg tip material is heat affected and charred, the pyrolysis gasses build pore pressure in the rubber material, and the material will try to expand. This expansion normally results in cracking of the charred material. If there is space for it to do so, the J-leg char will expand and bend other material around it.

In Figure 9, there is bent material that is the char of the mating surface. This char on the mating surface was bent by the heat effect that advanced through the J-leg tip. Remember that there were two surfaces that were heated – the J-leg tip surface and the mating surface. These two surfaces are positioned roughly 90° to each other.

In Figure 9, there is a fairly sharp corner of non-heat affected material between the two charred surfaces. If the heating events for both surfaces occurred at the same time, then this corner would be rounded – due to the effects of two dimensional heating. However, this sharp corner indicates that the heating events for the two surfaces occurred at different times. Normal J-leg tip heating occurs during all of motor operation. The observable post-fire char of the J-leg tip would be the result of normal motor performance.

It was understood that the char configuration in Figure 9 was indicating the timing of the heating event for the mating surface. Thermal models were created that could simulate the char configurations shown in Figures 3, 4, and 9. All scenarios were considered for the modeling effort. These models assumed a variety of boundary conditions for this attempt. With this effort, possibilities were examined as follows:

1) J-joint gas intrusion after motor operation and during re-entry: In this case, the models showed that there was not enough heat remaining in the motor after separation to reproduce the char thickness and configuration of the char observed in Figure 9.

2) J-joint gas intrusion early in operation and remaining open throughout motor operation: Thermal models were set up to simulate char formation in this scenario. In his case, the heating time would be extensive. Thermal models could not reproduce the char and pyrolysis depths observed in Figure 9 with this case. If 20 to 40 mils of char were to be produced in this long duration environment, then the pyrolysis depths would have been much greater than those observed on RSRM-55. The pyrolysis depths on RSRM-55 J-joints were very thin compared to the char depths. This kind of char and pyrolysis configuration can only be reproduced with a short duration but intense heating environment. So, this thermal model did not reproduce the effects seen.

3) J-joint gas intrusion late in operation: A variety of two dimensional models and conjugate flow models were created. This scenario would reproduce the relative char and pyrolysis depths observed. However, these models would not reproduce the sharp corner of non-heat affected material and the bent char layer on the mating surface. If the heating event happened late in motor operation, this material would have had heat approach it from two directions at the same time. In this case, the material would not have sharp corners. Instead, the material would be rounded as the two char fronts would increase the heat flux into this region by two dimensional conduction. So again, this thermal model did not reproduce the effects seen in Figure 9.

4) J-joint gas intrusion early in motor operation causing early heating with a short duration: In this scenario, the J-joint opens and the mating surfaces char severely early in motor operation. However, due to some condition (such as a decrease in J-joint deformation causing the J-leg to re-contact the clevis), the heating event stops shortly after it begins.

A variety of two-dimensional models were created to simulate this char pattern. The models predicted thick char relative to little pyrolysis depth. This result matched the condition in Figure 9. But, most importantly, these models also reproduced the sharp corner of non-heat affected material. The charring event happened early enough so that the rubber of the mating surface cools before the end of motor operation. Later in operation, as the inboard J-leg tip receives heating and swells, this heating would produce the sharp corner of unheated material trapped between the two surfaces. This thermal modeling approach did reproduce the effects seen in Figure 9.

Adding to evidence for the condition (4) above, is the bent char. The char on the mating surface would form, then cool, and then be bent by the subsequent J-leg tip heating and pore pressure.

This heating would start during the first 10 to 20 seconds into motor operation and be a short duration. The heating event would be shut down early in motor operation – likely just after 20 seconds – or maybe earlier. This heating scenario, at first glance, did seem unlikely because the following events would have to happen in sequence:

1) The PSA failed early
2) The J-joint opened to heat its mating surfaces
3) The J-joint then closed thereby shutting off the heating event early in motor operation
4) The char on the mating surfaces cooled
5) Late in motor operation, the cooled char on the mating surfaces were pushed away by the char swell in the J-leg tip.

As unlikely as this sequence seemed, it was the only heating event that could explain the char configuration in the samples like the one shown in Figure 9.

More collaborating evidence was needed. A structural assessment of the internal propellant grain and J-joint deformation was needed to explain this J-joint opening that was early and short in duration.

Structural Analysis Summary

By structural analysis, it was already understood that most of the J-joint deformation occurs during the first part of motor operation. Maximum deformation will be right after ignition (see Figure 5). This time is when the maximum clevis displacement occurs. If the J-leg remains adhered by PSA to the clevis, then this is when the J-leg experiences its maximum displacement (Figure 8a). If the inboard portion of the J-joint is not pressure actuated, then the J-joints could be pulled into tension during the first 10 to 20 seconds of motor operation. If the PSA is weak, then the J-joint may open as shown in Figure 8b. As motor operation time continues, the grain deformation subsides and the J-joint will decrease its deformation accordingly. After 20 seconds into operation, a J-joint can come back into compression due to the decrease in J-joint deformation.

An assembled J-joint is in compression in its pre-fired assembly state due to the interference fit. During storage time, the J-leg experiences some amount of compression set that reduces its inherent resiliency. During motor operation, if the J-leg does not remain mechanically attached to the clevis, as would be the case with failed PSA adhesion, the compression set of the J-leg will resist the movement of the J-leg back towards the clevis. During motor operation, there may be resiliency or relaxation that will help the J-leg come back into contact with the clevis (the view in Figure 8b would become the view in Figure 8a).

This structural assessment seemed probable. This assessment did collaborate the conclusion drawn by the thermal assessment – that is that the PSA failed early in motor operation (within the first 10 to 20 seconds) and the duration of the heating event was short (less than 20 seconds and maybe as short as 10 seconds)

Proof for PSA Failure Timing

Another static test motor was planned (FSM-8). The investigation team took this opportunity to prove the timing of the PSA failure and the duration of the subsequent heating event. But in order to prove this timing, internal instrumentation, which had never been previously used on an RSRM static test motor, would have to be designed and installed. This task would require special instrumentation wires exiting the large steel case pressure vessel. This effort would be no small accomplishment.

Internal instrumentation was developed for this full-scale static test. The instrumentation consisted of displacement gages and thermocouples positioned inside the static test motor J-joints. The instrumentation was arranged so that a J-joint PSA

failure would be detected. This instrumentation would detect the timing of a separation between the J-leg and clevis. The thermocouple was positioned in the interface between the J-leg and clevis, as shown in Figure 10. The installation of the thermocouple, which used 3 mil diameter wire, was done carefully and precisely so that its presence would not affect the operation of the J-joint. If the J-joint opened, this thermocouple would measure a temperature change and the time for that change. If the J-joint closed after heating, as was predicted, it would measure the time of that closure. A displacement gage was positioned in the insulation material adjacent to the J-leg as illustrated in Figure 10. This gage would measure relative displacement between the J-leg and the insulation surface. The idea was to measure both temperature and J-leg movement during J-joint opening caused by failure of the PSA. This instrumentation would either prove out the prevailing theory or provide data for a new theory.

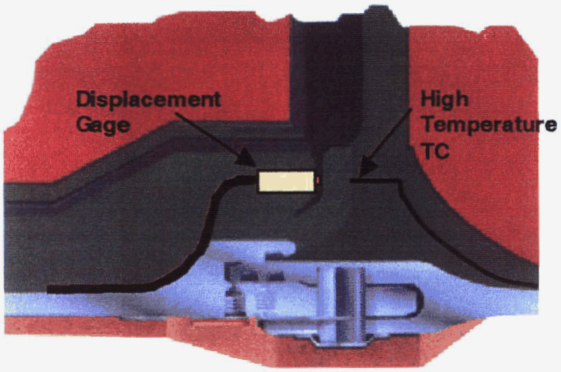

Figure 10. Thermocouple and Displacement Gage Placement in J-joint for Full-scale static Test

The conditions for J-joint assembly on RSRM-55 would have to be duplicated. The center J-joint was exposed to a "simulated" KSC humidity environment. The aft joint was needed for other test objectives on FSM-8, so it was not a part of this investigation. The center J-joint used the new PSA and ODC-free cleaning process under investigation. As was discussed above, the center J-joint experiences the most deformation. If the prevailing theory that the new PSA required both humidity and J-joint deformation to fail held true, then this instrumentation would record the start and duration of the event in the center J-joint.

The FSM-8 static test was fired (in February of 2000) and the instrumentation did indeed prove the main theory to be correct – that is, the center J-joint PSA failed early with a heating event that lasted for only a short duration. Figure 11 shows a plot of the J-joint thermocouple that recorded this event. This thermocouple did detect heating starting at 4 seconds and then ending at 11 seconds. The displacement data, although less conclusive, did show J-leg movement that would be indicative of this kind of J-joint reaction. These results supported the thermal and structural analysis predictions for an early but short heating event. In addition to the instrumentation data, post-test inspection revealed very similar charring characteristics as observed on RSRM-55 and FSM-7.

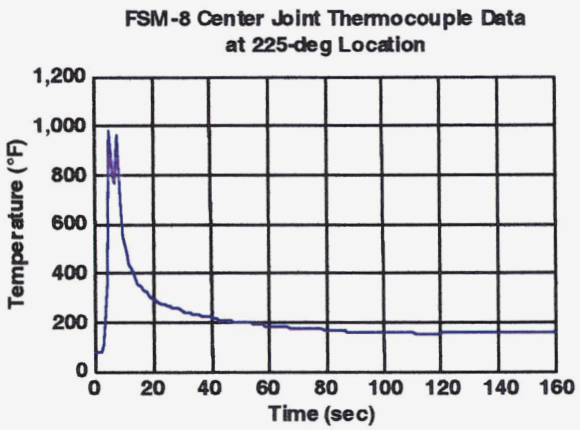

Figure 11. FSM-8 J-joint Thermocouple Data Showing Temperature vs. Time

CONCLUSIONS

The team now felt that they understood the parameters that would cause the new PSA to fail.

- The new PSA was the main root cause of the J-joint gas intrusion.
- In order for this new PSA to fail, there must be two other supporting failure causes as follows:
  - Prolonged J-joint exposure to KSC humidity,
  - J-joint motion that is experienced by the center and aft J-joints.

Along with these root causes, it was also understood that the inboard portion of the J-leg is not truly pressure actuated. Thus, the strength of the PSA is important – especially for the first part of motor operation where J-joint deformation and movement put the J-joint into tension.

Subsequent full-scale testing and flight data continue to confirm these conclusions. Two more static tests

have been completed which further demonstrated that the old (baseline) PSA would function properly in simulated KSC humidity. And, all RSRM flights using the baseline PSA have shown that this PSA functions properly with long exposures to humidity.

The following summarizes the J-joint gas intrusion and PSA failure scenario for RSRM-55:

1) The new PSA failed early in operation causing the J-joint to open.
2) The J-joint heating and charring resulted from this opening.
3) The J-joint closed shortly after the heating event started, thereby shutting off the heating event early in motor operation. The heating event was short in duration.

Future efforts to modify the J-joint assembly processes or to modify the J-joint materials (PSA) will have to consider the KSC humidity and temperature storage environments. The J-joint materials should be exposed to this type of environment during their testing.

LESSONS LEARNED

This experience of the development of a new PSA, its testing, the RSRM-55 flight, followed by the PSA failure investigation led to a good "lessons learned" list. At a glance, these lessons appear to be common sense. But these lessons are also easily forgotten.

First, a new design program must be sure to consider all loads and environments to which the product will be exposed. All environmental parameters should be considered – including parameters not previously considered to be a problem (such as long exposure to humidity). The axiom "test what you fly" is a good one.

Second, the designers must not assume that all of the physics are understood. Revisiting the assumptions of an older analysis is a healthy exercise. A reexamination of the physics should be done to better understand any unproven assumptions.

Last, if an unexpected event occurs, imaginative, resourceful, and creative testing and analysis can provide a simple explanation to what ordinarily appears to be a mystery.

ACKNOWLEDGEMENTS

The investigation team included many more individuals than the writers of this paper. This investigation was successful because of the hard work of many engineers, technicians, analysts and program managers.

The writers are indebted to many professionals in the ATK Thiokol Insulation Work Center. Many manufacturing technicians were involved with installing the insulation and instrumentation materials. The writers thank Todd Noble and his companions for their inventiveness in figuring a way to install rubber insulation with instrumentation. The writers thank Karl Kersker and the other lab technicians for their successful efforts in building test articles.

The writers thank the ATK Thiokol Propulsion Test Transducer Development Lab personnel. These technicians had a good working and positive attitude that led to many good ideas. These good ideas allowed many instrumentation successes along the way to the greatest success, which was internal instrumentation on a full-scale RSRM static test motor. Thanks goes to Lloyd Johnson, Alan Godfrey, and their co-workers for their feed-through development work and the careful installation of all instrumentation. Thanks especially goes to Boyd Bryner, their supervisor during this study.